# Biomolecule association rates do not provide a complete description of bond formation.

Philippe Robert, Laurent Limozin, Anne Pierres, Pierre Bongrand

**BIOMOLECULE ASSOCIATION RATES DO NOT PROVIDE A COMPLETE DESCRIPTION OF BOND FORMATION**

Philippe Robert[*†‡§], Laurent Limozin[*†‡], Anne Pierres[*†‡], Pierre Bongrand[*†‡§]

[*] INSERM UMR600, Lab. Adhesion & Inflammation, Parc Scientifique de Luminy, Case 937, 13288 Marseille Cedex 09, FRANCE
[†] CNRS UMR6212
[‡] Université de la Mediterranée
[§] Assistance Publique Hôpitaux de Marseille, Lab. Immunologie.

*Condensed title* : Biomolecule association rates

*Key words* : single-molecule studies, kinetics, diffusion, rough potential, molecular interactions

*Corresponding author*:  Pierre Bongrand, Tel (33) 491-82-88-52; Fax:(33) 491-82-88-51;
 E-mail: pierre.bongrand@inserm.fr.

**ABSTRACT**
The efficiency of many cell surface receptors is dependent on the rate of binding soluble or surface-attached ligands. Much effort was done to measure association rates between soluble molecules (3D $k_{on}$) and, more recently, between surface-attached molecules (2D $k_{on}$). The underlying assumption is that the probability of bond formation between receptors and ligands is proportional to the first power of encounter duration. Here we provide new experimental evidence and we review published data demonstrating that this simple assumption is not always warranted. Using as a model system the (2D) interaction between ICAM-1-coated surfaces and flowing microspheres coated with specific anti-ICAM-1 antibodies, we show that the probability of bond formation may scale as a power of encounter duration that is significantly higher than one. Further, we show that experimental data may be accounted by modelling ligand-receptor interaction as a displacement along a single path of a rough energy landscape. Under a wide range of conditions, the probability that an encounter of duration t resulted in bond formation varied as $\mathrm{erfc}[(t_0/t)^{1/2}]$, where $t_0$ was on the order of 10 milliseconds. It is concluded that the minimum contact time for bond formation may be a useful parameter in addition to conventional association rates.

## INTRODUCTION

The main function of proteins may be to bind to other biomolecules (1). In several situations such as antigen binding by antibodies (2), selectin-mediated tethering of leukocytes to the vessel walls on the onset of inflammation (3,4) or integrin activation (5,6), receptor efficiency is highly dependent on association rate; Measuring this parameter is thus considered as an important issue (7). Recently, many authors measured the rate of association between receptors and ligands in solution (8,9). Also, different techniques such as atomic force microscopy (10), fluorescence measurements (11), flow chambers (12) or micropipettes (13,14) yielded quantitative information on association rates between surface-bound molecules. It is now well recognized that it is difficult to relate association rates measured in solution (i.e. 3D conditions) to the behaviour of membrane-bound receptors (2D reaction) (7,15). However, all experiments relied on the assumption that it is possible to define an association rate parameter, $k_{on}$, such that the probability of bond formation between a ligand and a receptor maintained at binding distance during a sufficiently short time interval of duration t is proportional to t. The purpose of the present report is to show that this assumption may not be warranted in all experimental situations. In other words, $k_{on}$ cannot be used to predict bond formation under all conditions. First, we present experimental data supporting the view that the probability of ligand-receptor association may be proportional to a power of the contact time higher that one. It is argued that the problems related to the use of association rate were fairly unnoticed since i) encounter times between soluble molecules are set by diffusion rules and are therefore similar in all experiments, and ii) for practical reasons, binding experiments performed between surface-attached molecules at the single-bond level cannot be performed with a wide range of contact times. Second, we show that our findings are consistent with current theories of reaction rates. Third, we show that our experimental data are accounted for by a simple kinetic model based on a single parameter $t_0$ representing the minimum time required for bond formation. The probability of bond formation after a contact of duration t was $erfc[(t_0/t)^{1/2}]$, and $t_0$ was close to 10 ms.

## MATERIALS AND METHODS

**Particles and surfaces.** Tosylated microspheres of 4.5 µm diameter and 1,500 kg/m$^3$ density (Dynabeads M450, Dynal France, Compiègne) were coated with rat anti-murine immunoglobulin Fc (Serotec, France) then with mouse IgG1 anti human ICAM-1 (Ebiosciences, California, clone HA58) or control isotype (16). The surface density was estimated at 300 antibody molecules/µm$^2$ with flow cytometry and previously described calibration procedures (17).

Glass coverslips were covered with 200 µl of human Fc-ICAM-1 chimera (R&D systems) with a concentration ranging between 0.005 µg/ml and 0.02 µg/ml as previously described (16). The surface density of ICAM-1 group was estimated between 1 and 4 molecules /µm$^2$. Coverslips were then incubated with 10 µg/ml bovine serumalbumin in PBS to reduce nonspecific interactions. The total length of ligand and receptor molecules was estimated at 76 nm, approximating as 4 nm the length of an immunoglobulin domain (18).

The average distance d between a microsphere and the chamber floor was estimated with Boltzmann's law (15), yielding $d=k_BT/[(4\pi a^3/3)(\rho-\rho_0)g]$, where $k_B$ is Boltzmann's contant, T the absolute temperature, a the sphere radius, $\rho$ and $\rho_0$ are the sphere and medium densities and g is 9.81 ms$^{-2}$. The obtained estimate was 18 nm.

**Flow chamber and motion analysis**. We used published methods (19,20). Microspheres were driven in a flow chamber (6×20×0.1 mm$^3$) on an inverted microscope with a 20X objective. Images were acquired with a videocamera (Sony SPT-M 108CE, Japan), then digitized and DivX™ compressed with a WIN-TV digitizer (Hauppauge, France). Pixel size was (0.5 µm)$^2$. The centroid of microspheres was determined with a custom-made tracking program and trajectories were recorded with a time and space resolution of 20 ms and about 40 nm respectively.

A particle was defined as arrested when it moved by less than 500 nm during a time interval of 200 ms. A total of 94 independent experiments were performed, allowing us to record about 200 binding events, corresponding to between 25,000 and 140,000 positions, for each condition (i.e. shear rate and surface density of ICAM-1). The apparent duration of each arrest was corrected as previously explained (19,20) to derive an absolute arrest duration independent of the wall shear rate. The **binding frequency** f (per mm) was defined as the number of recorded binding events divided by the total trajectory length L of monitored particles. The statistical uncertainty was calculated as $(f/L)^{1/2}$ following Poisson law.

The frequency of specific binding under a given condition (i.e. wall shear rate and ligand surface density) was estimated by subtracting from the binding frequency measured with anti-ICAM-1 bearing spheres the result obtained with isotype controls. The statistical uncertainty of the difference was calculated as the square root of the sum of squared uncertainties. To ensure that sphere-to-surface distance was independent of the shear rate, we checked (not shown) that the ratio between the average particle velocity and flow rate remained constant as expected (21).

**Modelling the kinetics of bond formation between a ligand and a receptor molecule**.
**Model 1.**
The simplest model for the kinetics of bond formation between a ligand and a receptor molecules encountering each other is :

$$L + R \underset{k_{10}}{\overset{k_{01}}{\rightleftharpoons}} (LR)$$

(1)

Assuming that $k_{10}$ is much smaller than $k_{01}$, the probability P(t) that a ligand and a receptor will bind during a contact of duration t is simply given by :

$$dP(t)/dt = (1 - P(t))\, k_{01} \quad \Rightarrow \quad P(t) = 1 - \exp(-k_{01}t)$$

(2)

The **encounter efficiency** may be defined as the value of P(t) when t is the **encounter duration**. The **binding frequency** should thus be equal to the product of P(t) and the number $\lambda$ of molecular encounters per unit length of particle trajectory. Two limiting situations may be considered (5). If $k_{01}t$ is much higher than one, $P(t) \approx 1$ and binding frequency should be independent of particle velocity. Conversely, if $k_{01}t$ is much lower than unity, $P(t) \approx k_{01}t$ and binding frequency should be proportional to t. Measuring binding frequency will then yield an estimate of the association rate. Thus, a clearcut consequence of Model 1 is that **binding frequency should vary as a power of t comprised between 0 and 1**.

**Model 2.**
As shown on Fig. 1, a common way of refining model 1 consists of assuming that ligand-receptor association occurred as a two-step reaction as supported by previous studies (17,22,23):

$$L + R \underset{k_{10}}{\overset{k_{01}}{\rightleftharpoons}} (LR)_1 \overset{k_{12}}{\rightleftharpoons} (LR)_2$$

(3)

Assuming that state $(LR)_1$ is a transient complex with a lifetime intermediate between encounter time and 200 ms, thus remaining undetectable under our experimental conditions, and that $(LR)_2$ dissociation is negligible on this timescale, the probability of bond formation during encounter time t may be calculated as follows :

$$dP_0/dt = -k_{01}P_0 \ ; \ dP_1/dt = k_{01}P_0 - k_{12}P_1 \ ; \ dP_2/dt = k_{12}P_1 \qquad (4)$$

$$P(t) = P_2(t) = [k_{12}(1-\exp(-k_{01}t))-k_{01}(1-\exp(-k_{12}t))]/(k_{12}-k_{01}) \qquad (5)$$

Where $P_0(t)$, $P_1(t)$ and $P_2(t)$ are the probabilities of finding ligand and receptors respectively separated, in state 1 or in state 2, at time t after the onset of molecular encounter. An obvious limitation of this model is that Eq. 5 predicts that encounter efficiency **cannot** vary as a power of encounter time higher than 2, in contrast with experimental data (see results and Table 2 below). Note that this conclusion is not dependent on the neglect of $k_{10}$ that allowed marked simplification of kinetic equations without resulting in a marked change of theoretical binding plots. This limitation might be overcome by introducing a number of intermediate states $(LR)_3$, $(LR)_4$ ... in Eq. 3 (Fig. 1B). However, this would increase the number of adjustable parameters and still worsen the aforementioned difficulty in determining kinetic parameters.

**Model 3.**
We hypothesized that the introduction of a growing number of intermediate states might lead to a simple limiting scheme based on the concept of rough potential elaborated long ago (24,25) and well accepted now (26). The idea is that the multiple intermediate states may be accounted by modelling a molecular interaction as a diffusion along a reaction path with a low diffusion coefficient (Fig. 1C). Encounter efficiency could then be calculated as the proportion of diffusive complexes that reached a basin after a contact of duration t. Fick's law for one-dimensional diffusion of a particle with a diffusion coefficient D on a half line (x≥0) yields (27) :

$$\partial c(x,t)/\partial t = D \ \partial^2 c/\partial x^2 \ \Rightarrow \ c(x,t) = 1/\sqrt{(\pi Dt)} \exp(-x^2/4Dt) \qquad (6)$$

Where $c(x,t)$ is the probability density at time t and point x. The probability that a particle starting at x=0 will move by a distance higher than x after a period of time t is then obtained by mere integration, yielding $erfc(x/2\sqrt{(Dt)}$, where erfc is the error function complement (27).

**Numerical simulation of bond formation/dissociation**.
 Equation 6 does not describe accurately diffusion along actual energy landscapes. It was thus important to assess the robustness of this approximation. Since diffusion equations can be solved analytically only with a few simple conditions (27), we used numerical simulations to build data corresponding to a number of different energy landscapes. We modelled bond formation during an encounter of duration t as the random motion of a particle maintained during time t near the entry of a path made of a force-free segment with low diffusion coefficient (i.e. a kinetic trap) followed by an energy well representing the first detectable ligand-receptor complex. Bond formation thus occurred if the particle fell into the well during time t. The kinetic trap was modelled as a set of 100 sequential positions and the particle was allowed to jump at random from a position to an adjacent one at each time step with a low probability D that was directly related to the diffusion coefficient (15). The presence of a force F between positions (i) and (i+1) should thus increase the probability of jumping from (i) to (i+1) by $D\times[\exp(F) -1]$ in order to comply to Boltzmann's law. The results of non-dimensional simulation experiments could be fitted to experimental data by fitting parameters D and x, which amounted to chose a time and a length unit. However, as discussed above, encounter efficiency essentially depended on $Dt/x^2$. The validity of simulations was assessed by checking i) that the exact solution of Eq. (6) was closely fitted on a flat landscape (Fig. 7B) and ii) the relative probability of finding a particle at two close points near the center and the edge of an energy well (Fig. 7A) matched Boltzmann's law with less than 5% error after about 200,000 unit time steps.

**Estimate of the mean duration of molecular encounters**.

Defining as L the total length of ligand and receptor molecules, the time allowed for bond formation between a receptor moving at distance d from a ligand molecule with velocity w is $t = 2 (L^2 - d^2)^{1/2}/w$ (see Fig. 2). Since a receptor molecule M moving at distance z from a ligand-coated surface can interact with ligand molecules located in a strip of width equal to $2 (L^2 - z^2)^{1/2}$, the average encounter time may be approximated as :

$$<t_M>=(2/w) \int_0^{(L^2-z^2)^{1/2}} (L^2-z^2-x^2)^{1/2}/(L^2-z^2)^{1/2}dx=(\pi/2w)(L^2-z^2)^{1/2} \qquad (7)$$

The average interaction time was estimated by integrating over the microsphere region separated by a distance $\leq L$ from the surface and weighting with the probability for a point at height z to interact with a ligand, which is proportional to $(L^2-z^2)^{1/2}$:

$$<t>=(\pi/2w)\int 2\pi R\sqrt{(L^2-z^2)}\sqrt{(L^2-z^2)}dz/\int_h^L 2\pi R\sqrt{(L^2-z^2)}dz=$$

$$...= (\pi/6wL^2)[(2L+h)(L-h)^2]/[(1/2)Arccos(h/L)-(h/2L)(1-h^2/L^2)^{1/2}] \qquad (8)$$

Approximating L as 76 nm, h as 18 nm, and noticing that the relative velocity w between the surface of a sphere close to a plane in a shear flow is about 0.43 times the sphere velocity u (21), we obtain for the average molecular **encounter duration** :

$$<t> = 219/u \text{ (where t is in millisecond and u in } \mu m/s) \qquad (9)$$

Using an average encounter duration is only an approximation, but the accurate calculation of the distribution of encounter durations would result in awkward formulae without substantially changing the essence of our calculation.

**Estimate of the mean frequency of molecular encounters**.

As shown on Fig. 2B, a receptor located at M moving at distance z above a plane surface will encounter molecules located on a strip of width $2 (L^2 - z^2)^{1/2}$, where L is the length of the ligand+receptor couple. Defining as $\sigma_L$ the surface density of ligand molecules on the plane, the number of molecules encountered per unit time is $2 w (L^2-z^2)^{1/2} \sigma_L$. Integrating over the region of the microsphere surface located at binding distance from the plane, and noticing that the relative velocity between the sphere surface and the plane is 43 % of the sphere velocity, the number $\lambda$ of encounters per mm of sphere displacement is :

$$\lambda = \int_h^L (2\pi R\sigma_R)[2wt\sigma_L\sqrt{(L^2-z^2)}]dz$$

$$...= 4\pi R\sigma_L\sigma_R L^2 [(1/2) Arccos(h/L) - (h/2L) (1-h^2/L^2)^{1/2}] \qquad (10)$$

Where h is the distance between the sphere and the plane, and $\sigma_R$ is the surface density of receptors on the sphere surface (Fig. 2B). Taking as h the average sphere height as derived from Boltzmann's law and approximating L as 76 nm, we find $\lambda \approx 55,000$ mm$^{-1}$ when $\sigma_L$ is 2 $\mu m^{-2}$.

**Parameter fitting**.

Fitting experimental data to theoretical curves was achieved by minimizing the sum $S_{err} = \sum_i \ln^2(y_{exp}/y_{th})$ calculated on all experimental points; $y_{exp}$ and $y_{th}$ represent the experimental and calculated values of the encounter efficiency.

**Statistics**.

Analysis of variance and regression lines were obtained with standard statistical methods (28)

**RESULTS**

**Monitoring the formation and dissociation of single molecular bonds between ICAM-1 and anti-ICAM-1 antibodies**.

Microspheres of 2.25-µm radius were coated with anti-ICAM-1 antibodies and driven along ICAM-1-coated surfaces in a flow chamber. Based on Boltzmann's law, in accordance with direct measurements (16) the average distance between spheres and surfaces was estimated at 18 nm, much less than the total length of ligand receptor couples (about 76 nm). Thus, the duration of contact between ligand and receptor sites was limited by particle horizontal velocity rather than by vertical Brownian motion, in contrast with previously used conditions (15). The wall shear rate was varied between 14 and 98 $s^{-1}$, resulting in a mean particle velocity between 13 and 92 µm/s. The average time available for association between anti-ICAM-1 and ICAM-1 during an encounter (denominated as **encounter duration**) was thus estimated to vary between about 2.1 and 17 milliseconds.

Defining particles as arrested when they moved by less than 0.5 µm during a 200-millisecond interval, we detected numerous stopping events whose duration and frequency were recorded. Detachment rates are displayed on Table 1.

The hypothesis that these events were mostly mediated by single bonds is supported by the finding that i) **binding frequency** (i.e. number of arrests per unit length of microsphere displacement) was linearly dependent on the surface density of binding sites on the chamber floor (Fig. 3), ii) arrest duration was not altered when binding site density was varied, excepted with the lowest shear rate and highest binding site density where multiple bonds might occur during a same binding event (Table 1).

**The dependence of binding frequency on encounter duration is not consistent with a monophasic model including a single association rate parameter**.

A straightforward consequence of the standard model of bond formation described by Eqs 1 & 2 corresponding to model 1 of materials and methods is that binding frequency should scale as a power of encounter duration ranging between 0 and 1. As shown on Fig. 4, binding frequency scaled as a power of encounter duration higher than one. This conclusion could not be an artifact due to a low efficiency of bond detection at higher shear rate since ligand-receptor bond lifetime was not significantly shortened when the shear rate was increased (Table 1). Further, our conclusions are supported by previous reports from our and other laboratories (Table 2). Thus, bond formation between ICAM and anti-ICAM could not be modelled as a standard monophasic reaction.

**Accounting for experimental data with conventional kinetic models of multiphasic reactions would involve many unknown parameters that are difficult to derive unambiguously.**
A possible way of accounting for our data would be to assume that ligand-receptor association occurred as a multiphasic reaction involving transient intermediate complexes. The simplest case would involved a single transient state (see Fig. 1B and Eq 3, corresponding to Model 2 in Materials and Methods). Basic equations would yield two additional adjustable parameters as compared to Model 1 and provide the possibility that encounter efficiency might vary as a power of encounder duration lower than or equal to two.

  Experimental data were fitted to theoretical plots by varying two parameters, i.e. the number $\lambda$ of molecular encounters per mm of microsphere displacement and $k_{01}$, in order to minimize the sum of squared distances between the logarithms of experimental and calculated collision efficiencies (Fig. 5). The dependence of theoretical curves on $k_{12}/k_{01}$ was too weak to allow an accurate determination of the best choice for this ratio. The sum of squares ranged between 1.02 and 1.13. An obvious limitation of this model is that Eq. 5 predicts that encounter efficiency **cannot** vary as a power of encounter time higher than 2, in contrast with Fig. 4 and Table 2. This limitation might be overcome by introducing a number of intermediate states $(LR)_3$, $(LR)_4$ ... in Eq. 3. However, this would increase the number of adjustable parameters and still worsen the aforementioned difficulty in determining kinetic parameters.

Thus, the simple view that ligand-receptor association behaves as a monophasic reaction with a single on-rate parameter is unable to account for the behaviour disclosed by recent methods of dissecting ligand-receptor association at the single bond level. Further, the natural way of dealing with this situation by refining kinetic analyses (17, 22) is not fully convenient, even if it is often unavoidable, since this requires too many parameters to allow safe experimental determination of each of them.

**Experimental data perfectly match a simple model based on diffusion**.
As shown on Fig. 1C and described quantitatively in Materials and Methods, a simple model of bond formation between a ligand and a receptor maintained at binding distance during a short time t might consist of representing bond formation as a progression of the complex along a rough energy landscape involving multiple formation and dissociation of weak interactions. This suggests that encounter efficiency dependence on encounter duration might resemble the erfc function. As shown on Fig. 6, an excellent fit was found between binding frequencies and $\lambda$ erfc$[(t_0/t)^{1/2}]$ for the three tested surface densities of ICAM-1 molecules. The sum of squared errors was 0.21 at a density of 2 molecules ICAM-1/$\mu m^2$ and best fit parameters were $t_0$=8.94 ms and $\lambda$=27.5 encounters/mm. The same parameter $t_0$ and encounter frequencies of 27.5/2 and 27.5×2 mm$^{-1}$ respectively well fitted the experimental data corresponding to 1 and 4 ICAM-1/$\mu m^2$.

**Numerical simulations show that erfc provides a robust account of diffusion under a wide range of conditions.**
Since the simplified reaction pathway leading to erfc function may not closely mimic actual reaction pathway, it was important to know whether the analytical solution that matched our experimental results was strongly dependent on the shape of energy landscapes. Since diffusion equations can be solved analytically only for a limited numer or cases (27), extensive computer simulations were performed to explore the robustness of approximating diffusion with an erfc function. Representative results are shown on Fig.7. Conclusions may be summarized as follows :
i) The two-parameter function $\lambda$erfc$[(t_0/t)^{1/2}]$ often allowed a correct fit of the probability that a complex entering a reaction path at time zero will diffuse to an energy well after time t.

ii) Parameter $t_0$ is about $x^2/4D$, where x is the distance between the well and the entry of the reaction path, and D is the effective diffusion coefficient. Further, $\lambda$ should simply represent the frequency of molecular encounters per unit length of particle displacement.

iii) If the reaction well is too shallow, or if there is a high probability that the complex will exit from the reaction path before reaching the well, erfc may still give a correct account of encounter efficiency versus duration, but parameters $1/t_0$ and $\lambda$ may be markedly lower than $4D/x^2$ or the frequency of molecular encounters.

iv) That detachment rate increase did not result in significant decrease of arrest duration (Table 1) suggests that the binding state is sufficiently steep to resist hydrodynamic forces, according to the simple Bell model (29).

## DISCUSSION

The purpose of this work was to question the suitability of using an association rate constant ($k_{on}$) to describe the rate of bond formation between ligand and receptor molecules. The starting point was the experimental demonstration that the probability of bond formation during a molecular encounter of small duration t may be proportional to a power of t markedly higher than unity. A qualitative way of expressing this conclusion would be to state that bond formation requires a minimum contact time. Due to the significance of this conclusion, it is important to discuss the validity of all hypotheses underlying data interpretation.

**The decreased binding efficiency measured at higher shear rates cannot be due to a defect of arrest detection.** A simple explanation for our findings would be that binding events might be less efficiently detected at higher shear rate for two reasons : i) binding events should be shortened by the hydrodynamic drag supported by bonds ii) a very transient arrest might be less easily detected when the average velocity of unbound particles is higher, due to higher shear rate. These possibilities were ruled out by using low enough shear rates to avoid a substantial effect of forces on bond lifetime (Table 1) and only counting arrests much longer than the time resolution of our apparatus.

**The decreased binding efficiency measured at higher shear rate cannot be due to an increase of sphere-to-surface distance as a consequence of hydrodynamic forces**. We derived sphere height from velocity according to the four following steps:

i) We checked basic results from low Reynolds number hydrodynamics about the motion of a sphere close to a plane in a laminar shear flow (21). The dimensionless parameters h/R and u/RG (Fig. 2, h is the sphere-to-surface distance, R and u the sphere radius and velocity, and G the shear rate) are related through a universal relationship that was fitted to an analytical formula for convenience (15). While Reynolds number remained lower than $10^{-5}$, we had to assess the relevance of theoretical results to actual surfaces separated by nanometer-scale distances. As previously reported (15), we measured the velocity distribution of microspheres of 1.4µm and 2.25µm radius. We checked **without any parameter fitting** that G could be derived from velocity distribution with about 5% accuracy. Further, using known values of G and microsphere size and density, we showed that the calculated height distribution matched Boltzmann's distribution, thus supporting the view that forces generated during sphere-to- surface approach were much lower than the sedimentation force.

ii) As an **independent** check of the validity of hydrodynamic equations, we recently devised a method allowing direct measurement of the sphere-to-surface distance from images obtained with reflection interference contrast microscopy (RICM). Measurements were calibrated by studying the distance between a sphere glued to the tip of an atomic force microscope and a test surface. The method was then used for simultaneous determination of microsphere height and velocity in a

laminar flow chamber. It was concluded that the lubrication theory was acceptable with spheres of 2.25 µm radius and a wall shear rate of a few s$^{-1}$ (16).

iii) Then we used hydrodynamic equations to check that the sphere-to-surface distance h was independent of the flow rate as expected. In 76 independent experiments, we measured the ratio between the mean cell velocity and wall shear rate G (which was assumed to be proportional to the flow rate). First, we used analysis of variance to test the dependence of u/G on G: no correlation was detected (P=0.84). Second, we used standard linear regression methods to estimate the maximum admissible increase of (u/G) when G was increased from 28 to 98 s$^{-1}$, yielding 9.9% for a confidence threshold of 0.05 (28). The corresponding increase of sphere-to-surface distance h would be from 18 nm to 38 nm.

iv) The last step consisted of verifying that such an increase of parameter h could not account for the decreased binding efficiency we found at higher shear rates. According to Eqs (7-9), increasing h from 18 nm to 38 nm would decrease prefactor 219 of Eq. 9 by 14 %. The ligand receptor encounter time would thus be divided by 4.1 instead of 3.5 when the shear rate increased from 28 to 98 s$^{-1}$. This would not render the measured decrease of encounter efficiency accountable for by the linear model 1. Indeed, for all three surface concentrations of FcICAM we assayed, the respective decreases of contact efficiency were higher than 11 and 40 when the shear rate was increased from 28 s$^{-1}$ by a factor of 2.5 and 3.5 respectively.

**Validity of our estimate of contact duration**.

The interpretation of our results is dependent on the validity of Eq. 9 for two reasons. Firstly, we assumed that the duration of encounter between a ligand and a microsphere-bound receptor at height h was inversely proportional to the sphere velocity. Secondly, while the main point of our work was to demonstrate the lack of proportionality between contact duration and contact efficiency, our estimate of 10 ms for the order of magnitude of minimal contact time for bond formation was directly proportional to the prefactor 219 of Eq. 9. These assumptions are dependent on the three following points:

i) Local hydrodynamic forces might change the orientation of ligand and receptors, thus impairing contact formation at higher shear rate. This possibility was examined by modelling ligands and receptors as series of 2 or 3 rigid segments (Fig. 2C) and approximating the force and torque experienced by each segment as $6\pi\mu aGz$ and $4\pi\mu a^3G$, according to exact formulae obtained for spheres in viscous fluids (32). The sphere radius a was taken as half the length of considered segment, z was the distance between the segment center and the surface where it was anchored, the local value of G around molecules was approximated as the ratio between the relative velocity of the sphere surface and the sphere-to-surface distance. It was found that when z was higher than 29 nm the work of forces on segments during a right angle rotation was lower than $k_BT/10$, where $k_B$ is Boltzmann's constant and T is the absolute temperature. Further, ligand molecules separated from spheres by less than 29 nm were necessarily slanted even in absence of shear. Thus, the effect of hydrodynamic forces on the orientation of binding sites was deemed negligible.

ii) Eq. 7 assumes that ligand and receptor molecules are flexible enough to bind when the distance between their anchors ranges between about 18 and 76 nm. This point was addressed semi-quantitatively in a previous paper (30). Since binding sites are held by a total of three immunoglobulin molecules (Fig. 2C), thus providing three highly flexible hinge regions (31), Eq.7 should give an acceptable order of magnitude for <t>.

iii) Microspheres are subjected to a vertical brownian motion with an amplitude on the order of 18 nm, based on Boltmann's law. As mentioned above, the prefactor on Eq. 9 is only weakly dependent on microsphere height when this is less than about 50 nm. Thus, while brownian motion had a major influence on contact between microspheres of 1.4 µm radius and ligand coated surfaces (12, 15), this was not important under the experimental conditions used in the present experiments.

In conclusion, Eq. 9 should provide an acceptable approximation for the flow rate dependence and order of magnitude of ligand-receptor encounters.

**Our data are of general significance rather than reflecting a particular behaviour of the ligand-receptor couple used in this study**. In order to test the generality of our findings, we examined previously published reports on single bond formation between surface-attached molecules. As shown on Table 2, reported binding frequencies varied as a power of encounter time that might be much higher than unity.

**Which theoretical framework can be used to account for bond formation**.
The simplest way of accounting for an encounter efficiency scaling as a power of contact time between 1 and 2 may be to postulate the occurrence of an undetectable binding state with two additional adjustable parameters (Eq. 3 and model 2). Experimental data shown in Table 2 may be accomodated in this way with up to 5 intermediate stages (to account for exponent 4.5). However, there are two problems with this approach : i) it is not reasonable to derive more than two fitted parameters with a fairly simple-shaped experimental curve as shown on Fig. 2). ii) Even if this difficulty did not exist, it would be desirable to account for the binding behaviour of a given ligand-receptor couple with a limited number of parameters.

Thus, the growing number of parameters required to account for a number of experimental data (e.g. 19,22) by postulating the existence of an increasing number of barriers and basins in the energy landscape was an incentive for us to explore the possibility of using a simpler description by postulating the presence of a kinetic trap impeding the formation of the first stable complex. This hypothesis is supported by previous reports based on kinetic studies of protein conformational change, leading to the concept of rough energy landscapes (24-26).

**Conclusion**. While many authors emphasized the importance of association rates and reported difficulties in comparing 2D and 3D $k_{on}$, the suitability of this parameter to account for molecular interactions as conveniently as affinity constants or dissociation rates was not actually questioned. The data presented in this and other reports suggest that there is an intrinsic difficulty in using association rates to account for single bond formation between surface-attached molecules, and it is suggested that a possible way of dealing with this problem would be to postulate the existence of a kinetic trap resulting in threshold contact times for bond formation.

**REFERENCES**

1. Creighton TE (1993) *Proteins - Structure and Molecular Properties* (WH Freeman & Co, New York) 2nd Edition. 507pp.

2. Foote , Milstein C (1991) Kinetic maturation of an immune response. *Nature* 352:530-532.

3. Lawrence MB, Springer TA (1991) Leukocytes roll on a selectin at physiologic flow rates : distinction from and prerequisite for adhesion through integrins. *Cell* 65:859-873.

4. Dwir O, Kansas S, Alon R (2000) An activated L-selectin mutant with conserved equilibrium binding properties but enhanced ligand recognition under shear flow. *J. Biol. Chem.* 275:18682-18691.

5. Vitte J, Pierres A, Benoliel AM, Bongrand P (2004) Direct quantification of the modulation of interaction between cell-or surface-bound LFA-1 and ICAM-1. *J. Leukocyte Biol.* 76:594-602.

6. Zhang F, Marcus WD, Goyal NH, Selvaraj P, Springer TA, Zhu C (2005) Two-dimensional kinetics regulation of $\alpha_L\beta_2$-ICAM-1 interaction by conformational changes of the $\alpha_L$-Inserted domain. *J. Biol. Chem.* 280:42207-42218.

7. Dustin ML, Bromley SK, Davis MM, Zhu C (2001) Identification of self through two-dimensional chemistry and synapses. *Ann Rev. Cell Dev. Biol.* 17:133-157.

8. Schuck P (1997) Use of surface plasmon resonance to probe the equilibrium and dynamic aspects of interactions between biological macromolecules. *Ann. Rev. Biophys. Biomol. Structure* 26:541-566.

9. Leonard P, Säfsten P, Hearty S, McDonnell B, Finlay W, O'Kennedy R (2007) High throughput ranking of recombinant avian scFv antibody fragments from crude lysates using the Biacore A100. *J. Immunol. Methods* 323:172-179.

10. Hinterdorfer P, Baumgartner W, Gruber HJ, Schilcher K, Schindler H (1996) Detection and localization of individual antibody-antigen recognition events by atomic force microscopy. *Proc. Natl. Acad. Sci. USA* 93:3477-3481.

11. Dustin ML (1997) Adhesive bond dynamics in contacts between T lymphocytes and glass-supported planar bilayers reconstituted with the immunoglobulin-related adhesion molecule CD58 *J. Biol. Chem.* 272:15782-15788.

12. Pierres A, Feracci H, Delmas V, Benoliel AM, Thiéry JP, Bongrand P (1998) Experimental study of the interaction range and association rate of surface-attached cadherin 11. *Proc. Natl. Acad. Sci. USA* 95:9256-9261

13. Chesla SE, Selvaraj P, Zhu C (1998) Measuring two-dimensional receptor-ligand binding kinetics by micropipette. *Biophys. J.* 75:1553-1572

14. Chen W, Evans EA, McEver RP, Zhu C (2008) Monitoring receptor-ligand interactions between surfaces by thermal fluctuations. *Biophys. J.* 94:694-701.

15. Pierres A, Benoliel AM, Zhu C, Bongrand P (2001) Diffusion of microspheres in shear flow near a wall : use to measure binding rates between attached molecules. *Biophys. J.* 81:25-42.

16. Robert P, Sengupta K, Puech PH, Bongrand P, Limozin L (2008) Tuning the formation and rupture of single ligand-receptor bonds by hyaluronan-induced repulsion. *Biophys. J.* 95:3999-4012.

17. Pierres A, Benoliel AM, Bongrand P (1995) Measuring the lifetime of bonds made between surface-linked molecules. *J. Biol. Chem.* 270 : 26586-26592.

18. Fischmann TO, Bentley GA, Bhat TN, Boulot G, Mariuzza RA, Phillips SEV, Tello D, Poljak RJ. Crystallographic refinement of the three-dimensional structure of the FabD1.3-Lysozyme complex at 2.5-A resolution. *J. Biol. Chem.* 266:12915-12920.

19. Pierres A, Touchard D, Benoliel AM, Bongrand P (2002) Dissecting streptavidin-biotin interaction with a laminar flow chamber. *Biophys. J.* 82:3214-3223.

20. Pierres A, Prakasam A, Touchard D, Benoliel AM, Bongrand P, Leckband D (2007) Dissecting subsecond cadherin bound states reveals an efficient way for cells to achieve ultrafast probing of their environment. *FEBS Letters* 581:1841-1846.

21. Goldman AJ, Cox RG, Brenner H (1967) Slow viscous motion of a sphere parallel to a plane wall-II Couette flow. *Chem Engng Sci.* 22:653-660.

22. Beeson C, McConnell HM (1994) Kinetic intermediates in the reactions between peptides and proteins of major histocompatibility complex class II. *Proc. Natl. Acad. Sci. USA* 91 : 8842-8845.

23. Merkel R, Nassoy  P, Leung A, Ritchie K, Evans E (1999) Energy landscapes of receptor-ligand bonds explored with dynamic force spectroscopy. *Nature* 397:50-53.

24. Ansari A, Berendzen J, Bowne SF, Frauenfelder H, Iben IET, Sauke TB, Shyamsunder E, Young RT (1985) Protein states and proteinquakes. *Proc. Natl. Acad. Sci. USA* 82:5000-5004.

25. Zwanzig R (1988) Diffusion in a rough potential. *Proc. Natl. Acad. Sci. USA* 85:2029-2030.

26. Chu J W, Voth G A (2007) Coarse-grained free energy functions for studying protein conformational changes: a double-well network model. *Biophys. J*. 93:3860-3871.

27. Crank J (1975) *The mathematics of diffusion* (Oxford University Press, Oxford, 2nd edition) 414 p.

28. Snedecor, GW, Cochran W.G. 1980. Statistical Methods. Iowa State University Press, Ames, Iowa.

29. Bell G I (1978) Models for the specific adhesion of cells to cells. *Science* 200 : 618-627.

30. Pierres A, Benoliel A.M, Bongrand P (1998) Studying receptor-mediated cell adhesion at the single molecule level. *Cell Adhesion Communication* 5:375-395.

31. Valentine, R. C., Green NM. 1967. Electron microscopy of an antibody-hapten complex. J. Mol. Biol. 27:615-617.

32. van de Ven, T. G. M. 1989. Colloidal Hydrodynamics. Academic Press, London.

33. Paschall CD, Guilford WH, Lawrence MB (2008) Enhancement of L-selectin, but not P-selectin, bond formation frequency by convective flow. *Biophys. J*. 94:1034-1045.

34. Yago T, Zarnitsyna VI, Klopocki G, McEver RP, Zhu C (2007) Transport governs flow-enhanced cell tethering through L-selectin at threshold shear. *Biophys. J*. 92:330-342.

35. Edmondson KE, Denney WS, Diamond SL (2005) Neutrophil-bead collision assay : pharmacologically induced changes in membrane mechanics regulate the PSG-1/P-selectin adhesion lifetime. *Biophys. J*. 89:3603-3614.

36. Rinker KD, Prabhakar V, Truskey GA (2001) Effect of contact time and force on monocyte adhesion to vascular endothelium. *Biophys. J*. 80:1722-1732.

**TABLE 1**
**DETACHMENT RATE OF SURFACE-BOUND MICROSPHERES**

| ICAM-1 density | Wall shear rate | Detachment rate (second$^{-1}$) |
|---|---|---|
| 1 $\mu$m$^{-2}$ | 28 s$^{-1}$ | 0.54 $\pm$ 0.056 (n=274) |
| 2 $\mu$m$^{-2}$ | 28 s$^{-1}$ | 0.42 $\pm$ 0.029 (n=729) |
| 4 $\mu$m$^{-2}$ | 28 s$^{-1}$ | 0.27 $\pm$ 0.048 (n=165) |
| 1 $\mu$m$^{-2}$ | 56 s$^{-1}$ | 0.52 $\pm$ 0.087 (n=108) |
| 2 $\mu$m$^{-2}$ | 56 s$^{-1}$ | 0.44 $\pm$ 0.035 (n=543) |
| 4 $\mu$m$^{-2}$ | 56 s$^{-1}$ | 0.46 $\pm$ 0.071 (n=137) |
| 2 $\mu$m$^{-2}$ | 66 s$^{-1}$ | 0.57 $\pm$0.058 (n=267) |

Anti-ICAM-1 coated microspheres were driven along surfaces coated with ICAM-1 molecules at low density. The duration of binding events was recorded and used to derive the initial detachment rate $\pm$ statistical uncertainty as explained. The number n of recorded arrests is indicated in brackets.

**TABLE 2**
**INFLUENCE OF SHEAR RATE ON ENCOUNTER EFFICIENCY**

| Ligand/ receptor | Shear rate range ($s^{-1}$) | Relative shear increase $r_s$ | Relative binding efficiency decrease $r_b$ | exponent $\ln(r_b)/\ln(r_s)$ | reference |
|---|---|---|---|---|---|
| P-selectin Neutrophil | 20-100 | 5 | 10 | 1.43 | (33) |
| C-Cadherin C-Cadherin | 8.4-15.7 | 1.87 | 4.38 | 2.36 | (20) |
| L-selectin antibody | 40-50 | 1.25 | 2.8 | 4.5 | (34) |
| P-selectin Neutrophil | 25-200 | 8 | 42.5 | 1.8 | (35) |
| Streptavidin Biotin | 7.2-21.8 | 3.0 | 28 | 3.0 | (19) |
| Monocyte | 40-120 | 3.0 | 4.9 | 1.45 | (36) |

Published studies made on adhesion measurement under flow were used to derive the dependency of binding probability per encounter, denominated as encounter efficiency, on wall shear rate

**FIGURE LEGENDS**

**Figure 1: Models for the kinetics of bond formation. A)** Formation of a detectable bond as a biphasic process (model 2). Detectable ligand-receptor complexes (state2) are hypothesized to form through a unidimensional reaction path involving a transient undetectable state (1). The fraction of bound molecules (i.e. collision efficiency) may thus scale as the square of encounter duraton. **B)** When the reaction path involves multiple binding states, collision efficiency may scale as powers of encounter duraction higher than 2, requiring the use of an increasing number of parameters. **C)** A simple way of modeling a path involving multiple intermediate states may consist of using an "effective" diffusion coefficient with a low value on a segment of the reaction path that may be viewed as a "kinetic trap' (model 3).

**Figure 2: Geometrical parameters**. **A.** Motion of a microsphere near a planar surface in shear flow. The undisturbed flow velocity is Gz at distance z from the plane. The velocity u of the microsphere centre depends of the distance h between the sphere and the surface. The limiting ratio $\omega R/u$ is close to 0.57 when the sphere is close to the surface. The relative velocity w between the sphere surface and the plane is thus about 0.43 u. **B.** Bond formation may occur between points of the cell surface that are less than distance L from the plane. **C.** In order to assess the influence of confinement and hydrodynamic forces on molecular interactions, chamber bound molecules (anti-Fc+FcICAM) and microsphere receptors (anti-Ig + Ig anti-ICAM) were tentatively modeled as rigid rods connected with flexible hinge corresponding to the immunoglobulin hinge regions. Approximating as 4nm the length of an immunoglobulin domain, the lengths of segments s1, s2, s'1, s'2 and s'3 were respectively taken as 8nm, 36 nm, 8 nm, 16 nm and 8 nm.

**Figure 3: Linear dependence of binding frequency on ligand density**. Anti-ICAM-1-coated microspheres were driven along surfaces coated with ICAM-1 at low density with a wall shear rate of 28 $s^{-1}$ (squares) or 56 $s^{-1}$ (circles). The number of binding events per millimeter of trajectory is plotted versus ICAM-1 surface density. Vertical bar length is twice the standard error.

**Figure 4: Encounter efficiency is proportional to a power of encounter duration that is higher than unity.** Anti-ICAM-1-coated microspheres were driven along surfaces coated with a low density of ICAM-1 (1, 2 and 4 molecules/$\mu m^2$, shown with diamonds, squares and circles respectively) with a wall shear rate ranging between 14 and 98 $s^{-1}$. The frequency of specific binding events was plotted versus average duration of molecular encounters between ligand and receptor molecules, using a logarithmic scale. The slope of the regression line formed by the experimental values excluding the highest contact duration was respectively $2.41\pm0.18$, $2.88\pm0.32$ and $2.44\pm.30$ when ICAM-1 density was 1, 2 and 4 molecules/$\mu m^2$. Data found for 1 and 4 mol/$\mu m^2$ at 98 $s^{-1}$ (no significant binding) could not appear on a logarithmic scale.

**Figure 5: Standard kinetic modelling of encounter efficiency**.
The experimental dependence of binding frequency on wall shear rate was fitted to non-dimensional plots of encounter efficiency versus molecular contact duration expressed as the dimensionless product $k_{01}t$ (Eq. 5). A two-parameter fit was simply obtained by displacing the experimental curve on a log-log plot and minimizing the squared difference. Dot-segment, broken and thick curves were respectively obtained with $k_{12}/k_{01} = 10$, 1 and 0.1. The sum of squared errors corresponding to the best fit was $1.08 \pm0.06$ for all curves, demonstrating the impossibility of unambiguously determining $k_{12}/k_{01}$. There was a large uncertainty in locating the adjusted data (squares) since the best-fit regions of calculated curves closely matched a straight line with a slope of 2 and fitted values of $\log(k_{01}t)$ could be indefinitely decreased without significantly altering the

squared difference.  The accuracy of the fit is illustrated by considering a slightly translated curve (triangles) yielding a sum of squared errors of 2.50.

**Figure 6: Excellent match between erfc and experimental data.**
The plots of binding frequency versus estimated contact duration (Eq. 2) were fitted to erfc ($t^{-1/2}$) by dividing all abscissae by the same factor of 8.94 ms and frequencies by 13.75, 13.75×2 and 13.75×4 mm$^{-1}$ respectively when the surface density of ICAM-1 was 1 µm$^{-2}$ (diamonds), 2 µm$^{-2}$ (squares) and 4 µm$^{-2}$ (circles) respectively.

**Figure 7: Many models based on the "kinetic trap" assumption lead to an erfc-like relationship between encounter efficiency and contact duration.**
**A.** *Typical simulation*. The **reaction path** was modelled as as sequence of 100 positions with energy shown on *top curve*. A sink was located at position 0 to account for more stable inner binding states. A particle starting from position 100 was considered as bound after N **steps** if it moved leftward by at least distance x. Fall into the sink was slowed by a wide barrier of 4 kT. Complex entry into or exit from the reaction path (at position 100) was modelled as a random exchange with a reservoir on the right. *Bottom*: the probability distribution of a particle starting from position 100 at time 0 is shown after 1000 time steps (Thick line), 10,000 steps (thin line) and 100,000 steps (broken line) respectively. **B.** ***Results of simulation.*** *Diamonds* show simulated binding probabilities for a flat energy landscape with a sink at position zero and a barrier preventing exit at position 100. the thin line represents the exact solution of diffusion into a half line, i.e. erfc[$(x^2/4Dt)^{1/2}$]. The discrepancy after 100,000 steps is due to the passage into the sink. *Squares* show the effect of replacing the flat energy landscape with the curve on Fig.5A (top). The thin line shows that experimental curves can still be fitted to an erfc function with a different timescale. Circles show the effect of allowing particles to exit rightward from the reaction path (with a probability of going back one hundredfold lower). The simulated data are still matched with an erfc curve with different scaling parameters.
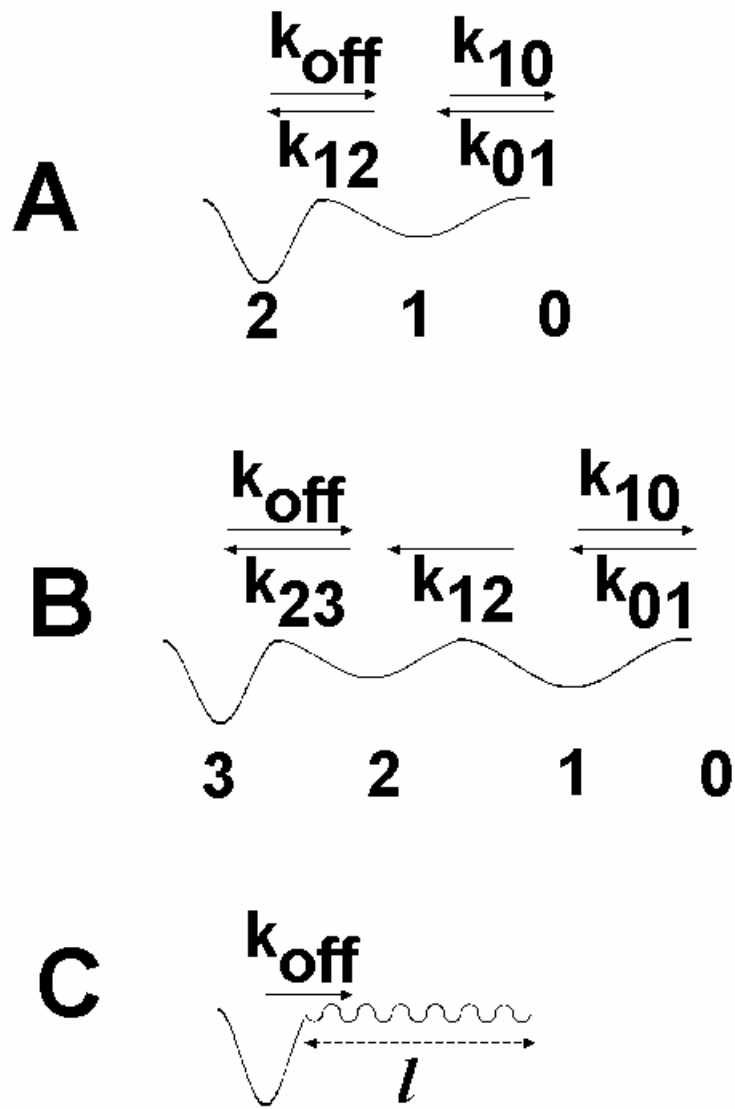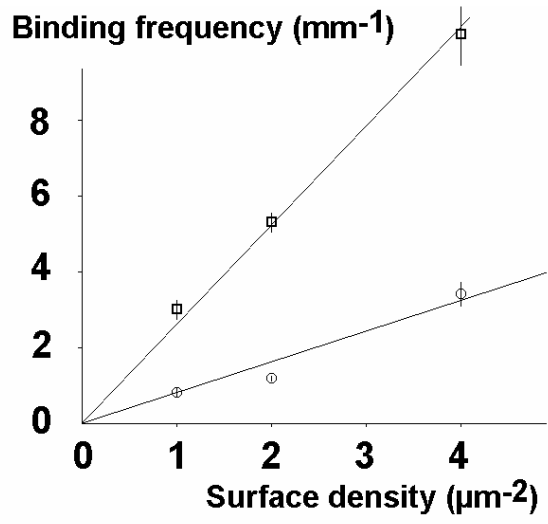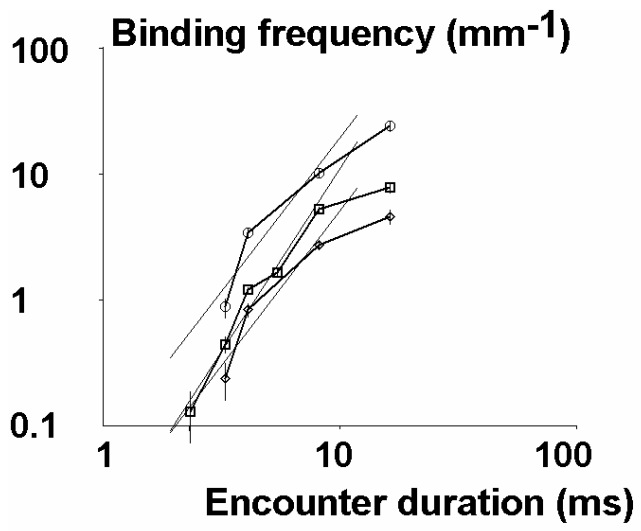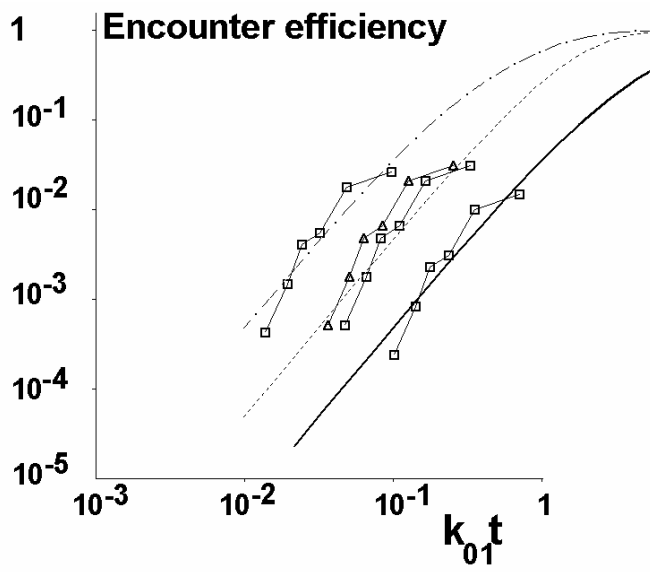
Figure 1

Figure 2

Figure 3

Figure 4

Figure 5

Figure 6

Figure 7